AN ANALYSIS OF BLADE-MOTION STABILITY FOR AN ARTICULATED ROTOR

By Julian L. Jenkins, Jr.

NASA Langley Research Center
Langley Station, Hampton, Va.

Presented at the 24th Annual National Forum of
the American Helicopter Society

Washington, D.C.
May 8-10, 1968

AN ANALYSIS OF BLADE-MOTION STABILITY FOR AN ARTICULATED ROTOR

Julian L. Jenkins, Jr.
Aerospace Technologist
NASA Langley Research Center
Langley Station, Hampton, Va.

Summary

The blade-motion stability of a fully articulated rotor (i.e., flapping and lead-lag degrees of freedom) is evaluated using a numerical solution to the coupled, nonlinear equations of motion. Two effects of initial conditions on the tip-speed ratio for divergence are indicated by varying the initial azimuth position for introducing a disturbance and by varying the disturbance amplitude at the critical azimuth angle.

Methods of extending the divergence boundary of an articulated rotor are examined. The effects of hinge restraint (e.g., spring and damping) and flapping hinge cant angle δ_3 are evaluated individually and a representative combination of these parameters was chosen to indicate the overall effect on blade-motion stability.

Introduction

The evolution of the helicopter from the low-speed utility aircraft to a high-speed, high-performance system is progressively placing the rotor in a more extreme environment wherein stall and compressibility effects seriously reduce performance. Compounding, by the addition of wings and auxiliary propulsive systems, permits the rotor loading to be reduced to minimize stall effects; however, when the rotational speed of the rotor is reduced in order to limit the advancing blade Mach number, the operating tip-speed ratio rises rapidly. The increase in the operating tip-speed ratio places the rotor in a regime wherein blade-motion stability becomes a matter of extreme importance.

As has been demonstrated by numerous investigations, rotor blade-motion stability is of critical concern at tip-speed ratios above 1.0 (see, for example, refs. 1 to 4). Each of the cited references has indicated tip-speed ratios for which the blade motion becomes divergent; however, as is the case for any dynamic system, the stability is in part a function of the initial conditions imposed as a disturbance. In addition, the design parameters of the rotor hub system can affect the stability of the rotor.

It is the purpose of this paper, therefore, to examine the effect of the initial disturbance on blade-motion stability and to explore various methods for extending the operating tip-speed ratio of the rotor. The methods include spring and damper restraints and δ_3. Some preliminary results of the effects of initial conditions on rotor stability were presented in references 3 and 4. The equations of motions used in this study are also presented in reference 4.

Presented at the 24th Annual National Forum of the American Helicopter Society, May 1968.

L-6088

Symbols

c	blade section chord, ft
e_1	offset of center line of flapping hinge from center line of rotor shaft, ft
e_2	offset of center line of lead-lag hinge from center line of flapping hinge, ft
$e_t = e_1 + e_2$, ft	
I_F	equivalent mass moment of inertia of blade about flapping hinge, $\int_{e_1}^{R} m(r - e_1)^2 dr$, slug-ft^2
I_h	mass moment of inertia of e_1 blade about lead-lag hinge, $\int_{e_t}^{R} m(r - e_t)^2 dr$, slug-ft^2
K_{SF}	flapping spring constant, lb-ft/rad
K_{SL}	lag spring constant, lb-ft/rad
m	mass of blade per unit radius, slugs/ft
r	distance measured along blade from axis of rotation to blade element, ft
R	total radius of undeflected blade, ft
V	velocity along flight path, ft/sec
β	blade flapping hinge angle, rad
γ'	mass constant of rotor blade, $\rho c R^4 / I_h$
δ_3	blade flapping hinge cant angle, deg
ζ	blade leading angle, rad
ξ	damping ratio
ρ	mass density of air, slugs/ft^3
ψ	blade azimuth angle, measured from downwind position in direction of rotation, deg or rad as indicated
ω_n	natural frequency, rad/sec
Ω	rotor angular velocity, rad/sec

Subscripts:

0	initial condition

F referred to flapping axes

L referred to lag axes

Analysis

The results presented herein were obtained from a digital solution of the coupled, nonlinear equations of motion for the fully articulated rotor hub system (i.e., flapping and lead-lag degrees of freedom) illustrated in figure 1. The equations are derived and presented in reference 4. Also included in the reference is the procedure used to determine the stability of a given configuration. The same procedure was used herein. The procedure was to select a configuration and then introduce an initial disturbance on the flapping angle at a specific initial azimuth angle. Input parameters which would introduce a forced response of the flapping motion were maintained at zero so that the solution obtained represents the transient solution of the equations of motion. With this procedure, the flapping angle converged to zero amplitude for stable conditions and the lag angle achieved a steady-state forced response. In order to minimize the effects of compressibility, the rotational speed of the rotor was reduced as airspeed was increased so as to maintain an advancing tip Mach number of 0.8 for all tip-speed ratios.

As was the case for the boundaries presented in both references 3 and 4, the stability boundaries presented herein represent boundaries where one or both of the angles (i.e., β or ζ) exceed 90°. Thus, even though the motion is stable on one side of the boundary, the amplitudes allowed near the boundary are not tolerable from the standpoint of practical operation.

Results and Discussion

Earlier studies have indicated that rotor blade-motion stability boundaries cannot be rigidly defined. References 3 and 4, for example, indicated significant changes in the tip-speed ratio for divergent motion as either the magnitude or initial azimuth angle of the disturbance was altered. Figure 2, which was taken from reference 4, shows regions of stable and unstable blade motion as functions of the blade mass constant and tip-speed ratio for two different initial conditions. Since the mass constant parameter is inversely proportional to the blade inertia, light blades are at the upper end of the scale and heavy blades are at the lower end. The increment in tip-speed ratio between the two boundaries illustrates the large effect of the initial azimuth on the blade-motion stability. As the mass constant decreases by increasing the blade mass, the effect of initial azimuth is not as large; however, rotor blades generally have a mass constant in the range from 1.0 to 2.0 where a sizable increment in tip-speed ratio exists.

Effect of Initial Azimuth Angle

In order to determine the variation of the stability boundary for various initial azimuth angles, a representative mass constant of 1.6 was selected and an initial flapping angle disturbance of 0.2 radian was introduced around the rotor disk. The resulting variation in the boundary is presented in figure 3. The boundary shows a sizable increment in the tip-speed ratio for divergent motion between the advancing and retreating sides of the disk. As expected, the most critical area is in the second quadrant (i.e., $\psi_0 = 90^\circ$ to 180°) wherein the blade encounters a destabilizing aerodynamic spring force and high dynamic pressure. The boundary on the retreating side of the disk shows very little effect of variation in initial azimuth; however, as indicated by the shaded area between $\psi_0 = 180^\circ$ and $\psi_0 = 340^\circ$ there exists a small range wherein the blade motion was neutrally stable. In effect, the motion represents a limit cycle instability in that the blade motions neither converge nor diverge.

Effect of Initial Disturbance Amplitude

In figure 3, an azimuth angle of approximately 90° represented the most critical area for introducing an amplitude disturbance.

It is of interest to examine the effect of the initial flapping amplitude used to initiate the transient. The variation in the stability boundary for a range of initial flapping amplitudes is presented in figure 4. The result indicated that the rotor blade motion is convergent at higher tip-speed ratios as β_0 is reduced. A comparison of figures 3 and 4, shows that a disturbance angle of less than 0.02 radian is required to achieve the same level of stability indicated for a 0.2-radian disturbance introduced on the retreating side of the rotor disk.

As a consequence of the shifts in the stability boundary which occur for varying initial conditions, there would appear to be a range of tip-speed ratios wherein the rotor could operate as long as it encountered no significant disturbances. If, however, a disturbance of sufficient magnitude was encountered at the appropriate azimuth position, the blade motion could rapidly diverge.

Methods of Extending Blade-Motion Stability Boundaries

The mechanism whereby a rotor encounters destablizing aerodynamic spring forces in the forward quadrants of the rotor disk was illustrated and discussed in reference 3. It was pointed out that increasing the hinge restraints by the addition of structural stiffness or dampers or decreasing the aerodynamic spring by incorporating blade pitch-flap coupling should provide means for extending the divergent tip-speed ratio. Several of these methods are examined herein. The parameters considered are spring and damper restraints and flapping hinge cant angle δ_3. Each parameter is considered individually and then a specified combination of the parameters is evaluated.

Flapping Hinge Restraint

Spring restraint. The addition of spring restraint to the flapping hinge is somewhat analogous to replacing the hinge with a structural flex plate. The spring stiffness has been added herein without regard to structural integrity of the system. Such considerations could compromise the improvements illustrated in figure 5. The spring stiffness is presented in terms of the flapwise natural frequency ratio as determined from the following expression:

$$\left(\frac{\omega_n}{\Omega}\right)_F = \left(1 + \frac{K_{SF}}{I_F \Omega^2}\right)^{1/2}$$

It should be pointed out that the spring rate K_{SF} was adjusted to maintain a constant frequency ratio as the rotational speed was decreased. The rotational speed was reduced so as to maintain an advancing tip Mach number of 0.8 throughout the range of tip-speed ratios.

The results indicate a nearly linear increase in the divergence boundary with increasing frequency ratio. For ratios from 1.0 to approximately 1.5 the blade flapping hinge motion diverges, whereas above 1.5, the lagging motion is initially divergent. This change in the mode of divergence apparently results from the Coriolis acceleration terms in the lead-lag equation of motion reaching magnitudes large enough to cause very large inplane amplitudes. As evidenced by the decrease in effectiveness of the spring at the higher frequency ratios, the lag disturbance is apparently approaching a critical level which causes a very rapid divergence of the lag motion.

Damping restraint. The effect of increasing flapwise damping by the addition of a viscous damper at the flapping hinge is shown in figure 6. The results indicate a rapid improvement in the divergence boundary for up to 20 percent of critical damping. Above 20 percent the increased damping does not produce any substantial increase in the divergence tip-speed ratio. The decrease in flapping damper effectiveness is again due to the buildup in amplitude of the inplane motion until it becomes the divergent mode. Even though there is adequate damping to prevent a flapping motion divergence, the initial flapping response produces inplane Coriolis accelerations large enough to cause divergence similar in nature to that which occurred with a stiff flapping spring.

A comparison of figures 5 and 6 indicates that the flapping spring restraint is more effective than the damping restraint for extending the divergence boundary. This results partially from the capability of the spring restraint to reduce the flapping velocity more effectively than does the flapping damper. Thus, the rotor may be operated at higher tip-speed ratios before the inplane excitation reaches sufficient magnitude to cause an inplane divergence.

It is apparent from the results presented in this section that realization of the total benefit of either type of flapping restraint will require an inplane restraint. These restraints are investigated in the following section.

Lead-Lag Hinge Restraint

Spring restraint. The effect of increasing lead-lag hinge spring restraint on the divergence boundary is presented in figure 7. The results are presented as a function of the inplane frequency ratio as determined from the following expression:

$$\left(\frac{\omega_n}{\Omega}\right)_L = \left[\frac{3}{2}\frac{e_2}{R - e_t}(1 + n)\right]^{1/2}$$

where

$$n = \frac{K_s}{\frac{3}{2} I_h \frac{e_2}{R - e_t} \Omega^2}$$

The basepoint of the boundary occurs at a frequency ratio of 0.28 which corresponds to the basic inplane natural frequency for a 0.05R lag hinge offset.

As the inplane stiffness increases, there is an initial improvement in the divergence boundary; however, as the frequency ratio approaches 1.0, the tip-speed ratio for convergent motion is reduced significantly. Above a frequency ratio of 1.0, the boundary again shows an improvement. At frequency ratios approaching 2.0, the blade undergoes a pure divergence in the flapping mode. This type of nonoscillatory divergence will be discussed further in the section considering lag hinge damping restraint.

Accompanying the reduction in the divergence boundary for frequency ratios near 1.0, was an area where a "limit cycle" instability was encountered. The area is outlined in figure 7. The blade-motion characteristic of points established in this area was a steady-state, 1/2 per rev flapping response. There is, of course, the possibility of other such areas existing, but with the numerical technique used herein, it is not feasible to define them without prior knowledge of the approximate condition required.

Damping restraint. The results obtained for the addition of an inplane damper are presented in figure 8. The trends indicated are similar to those obtained with the addition of flapping hinge damping (see fig. 6). The mode of divergence differs, however, for the two cases. As mentioned previously, the effectiveness of the flapping hinge damper is limited by the inplane divergence for damping ratios above 0.2, whereas the boundary for lag damping results in all cases from a divergent flapping mode. In fact, above a damping ratio of 1.0, the blade flapping motion undergoes a pure divergence (i.e., nonoscillatory) when released with the specified initial conditions as was also

the case for the lag hinge spring restraint. The boundaries established for either lag hinge spring restraint or damping restraint appear to be approaching an asymptote which is in the region of the flapping divergence boundary established for a single-degree-of-freedom, flapping rotor. As pointed out in reference 2, complete flapping instability occurs at a tip-speed ratio of approximately 2.0 for a blade with the mass factor used herein.

Effect of Flapping Hinge Cant Angle

Blade pitch-flap coupling represents one of the simplest feedback mechanisms which can be incorporated on a rotor. Since its function is to reduce blade loading with increased flapping angle, it may be considered as being analogous to increased spring stiffness. The spring constant is nonlinear since the aerodynamic forces produced are a function of both blade azimuth position and tip-speed ratio. In addition, in the reverse velocity region, the effects of positive δ_3 are reversed and thus produce a negative spring effect. Nevertheless, increasing the flapping hinge cant angle provides a very effective method for extending the divergence boundary as is illustrated in figure 9.

A comparison of the boundary for flapping hinge spring restraint (fig. 5) and the boundary in figure 9 indicates that approximately 40° of δ_3 is equivalent to doubling the frequency ratio by increasing spring restraint. Since flapping hinge cant is not a physical restraint as is the spring stiffness, it is quite probable that its potential may be more fully utilized as compared to blade root restraint with its attendant increase in stress.

Effect of Selected Combination of Parameters

In order to assess the overall effectiveness of combining methods for extending the stability boundary, a selected combination of the design parameters was evaluated and compared with the total extension which would be expected if the individual increments could be added linearly.

The rotor hub characteristics selected for this evaluation and the approximate increment achieved on an individual basis are shown in the following table:

	$\Delta V/\Omega R$
Flapping spring restraint . . . $\omega_n/\Omega = 1.2$	0.3
Flapping damper restraint . . . $\zeta = 0.2$	0.5
Lag hinge restraint . . . . . $\omega_n/\Omega = 0.6$	0.3
Lag damper restraint . . . . . $\zeta = 1.0$	0.7
Flapping hinge cant angle . . . $\delta_3 = 30^\circ$	1.3
	3.1

Again, the indicated frequency and damping ratios were maintained as rotational speed was reduced by adjusting the spring and damper constants. The total increment from the preceding table is $\Delta V/\Omega R = 3.1$. This increment, plus the baseline tip-speed ratio of 1.4, indicates an extension of the divergence boundary to $V/\Omega R = 4.5$.

The combined parameters did not produce the total extension which might be anticipated on the basis of the linear combination of the individual increments. In fact, the flapping amplitude exceeded the 90° criterion at a tip-speed ratio of approximately 4.1. This would infer that some of the restraints selected may not be needed in order to achieve the same extension in the divergence tip-speed ratio.

It would appear that the combination of parameters selected would provide a rotor system with a high degree of stability, particularly in view of the relatively large artificial disturbance used to initiate the transient. In view of the various stabilizing devices, the response to disturbances such as gusts should not be as large and therefore the blade-motion amplitudes would be less likely to exceed the value required to produce a divergent condition.

As previously mentioned, the damping and spring constants were varied in order to maintain the desired frequency and damping ratios. In practice, however, changing rotational speed will also change both the frequency ratio and the damping ratio about the two hinges. In order to assess the effect of changing frequency and damping ratios as the rotor rotational speed is reduced, the spring and damper constants were selected such that the frequency and damping ratios indicated in the preceding table are valid at a tip-speed ratio of 1.0. With the constants fixed in this manner, the tip-speed ratio was progressively increased until the blade motion became divergent.

The results are presented in figure 10 as a boundary showing the effect of initial disturbance amplitude. Also included is the boundary from figure 4 for the basic rotor without hinge restraints or δ_3. The data indicate that the constrained rotor is stable for tip-speed ratios four to five times as high as the basic rotor. This large difference in the divergence boundaries should also be indicative of a reduction in the response sensitivity at lower tip-speed ratios.

Response Sensitivity of a Constrained Rotor

As an example of the reduction in blade-motion response which may be achieved by incorporating hub restraints, the rotor system defined in the preceding section was subjected to angle-of-attack step inputs and the maximum peak-to-peak amplitude of the ensuing motion was obtained. The results are presented in figure 11. The response of the rotor without restraints is also included for comparison.

The data in figure 11 indicate a sizable reduction in amplitude of the transient response for the constrained rotor as compared to the basic rotor. If, for example, 15° amplitudes represented the point at which the blade would strike

the flapping stops, the basic rotor would reach this limit with very small disturbances. On the other hand, the constrained rotor does not exceed an amplitude of 10° for a 6° change in angle of attack. Since an angle-of-attack change of 6° is equivalent to a vertical gust of approximately 47 ft/sec, the constrained rotor would have to be subjected to the most extreme disturbance before encountering the 15° limit. Again it should be pointed out that the restraints have been incorporated without consideration of the structural aspects, which could, of course, place a more stringent requirement on the acceptable transient amplitudes.

Concluding Remarks

The blade-motion stability of a fully articulated rotor has been examined using a numerical solution to the coupled, nonlinear equations of motion. The results indicate that variations in the magnitude or initial azimuth of the disturbance amplitude can produce large changes in the tip-speed ratio for divergent motion.

Methods of extending the divergence boundary were also examined. Spring or damping restraint on either of the flapping hinge or the lag hinge were shown to be effective methods. The effectiveness of these types of constraints may be limited by the structural integrity of the system. Flapping hinge cant angles δ_3 also proved to be effective in delaying divergence and from the standpoint of structural considerations could be utilized more fully than the physical restraints such as the springs and dampers.

A combination of the individual restraints increased the divergence boundary to tip-speed ratios four to five times as high as the unconstrained rotor. In addition, the flapping response to vertical gusts was reduced by over 75 percent at a tip speed of 1.0 as a result of the restraints used.

References

1. Horvay, Gabriel, Rotor Blade Flapping Motion, Quart. Appl. Math., July 1947.

2. Jenney, D. S.; Arcidiacono, P. J.; and Smith, A. F., A Linearized Theory for the Estimation of Helicopter Rotor Characteristics at Advance Ratios Above 1.0, Proceeding of the 19th Annual National Forum of the American Helicopter Society, May 1963.

3. Jenkins, Julian L., Jr., Calculated Blade Response at High Tip-Speed Ratios, Conference on V/STOL and STOL Aircraft, NASA SP-116, 1966.

4. Jenkins, Julian L., Jr., A Numerical Method for Studying the Transient Blade Motions of a Rotor With Flapping and Lead-Lag Degrees of Freedom, NASA TN D-4195, 1967.

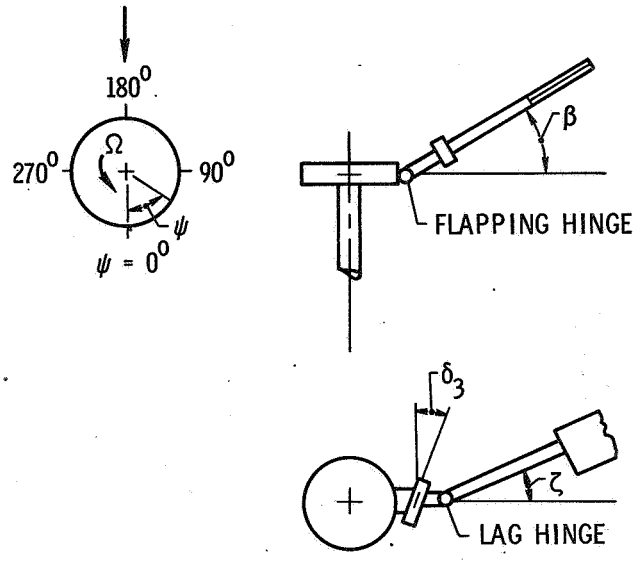

Figure 1.- Rotor hub geometry.

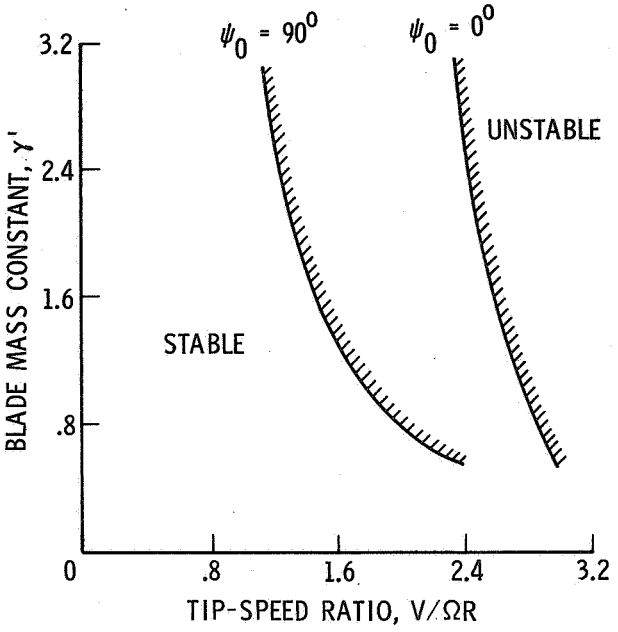

Figure 2.- Effect of blade mass constant on blade-motion stability.

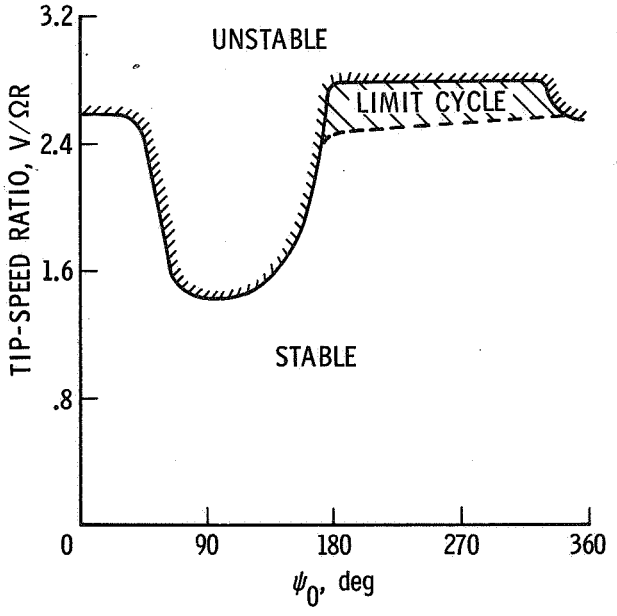

Figure 3.- Effect of initial azimuth angle on blade-motion stability. β_0 = 0.2 rad.

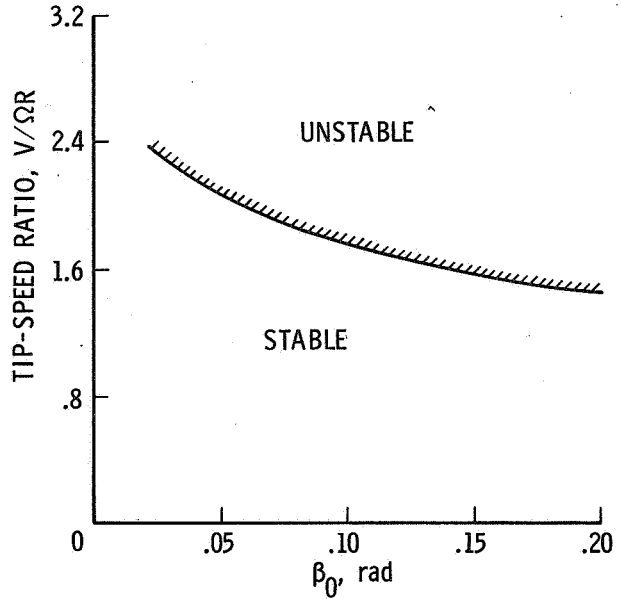

Figure 4.- Effect of initial disturbance amplitude on blade-motion stability. $\psi_0 = 90°$.

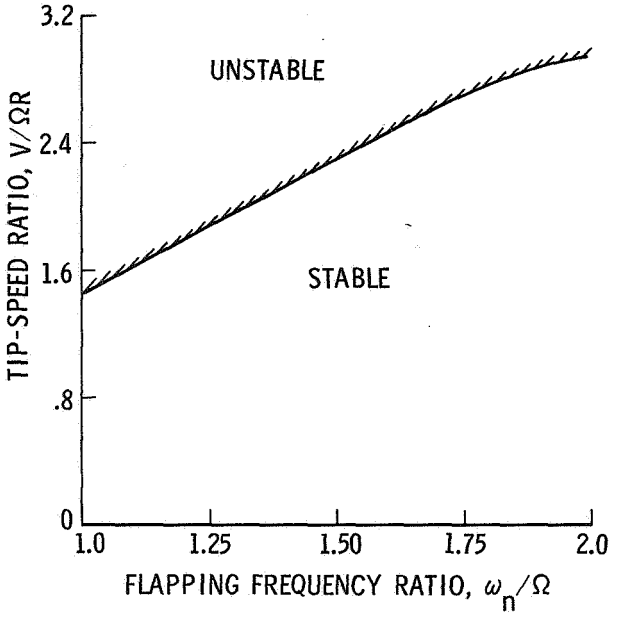

Figure 5.- Effect of flapping hinge spring restraint.

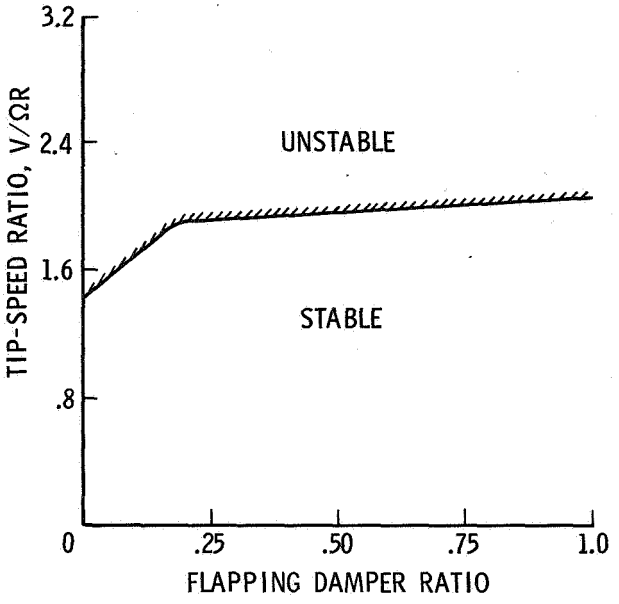

Figure 6.- Effect of flapping hinge damper restraint.

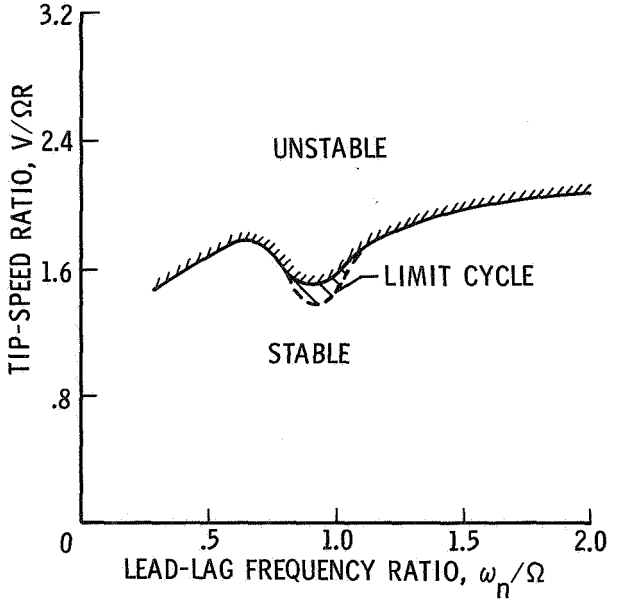

Figure 7.- Effect of lead-lag hinge spring restraint.

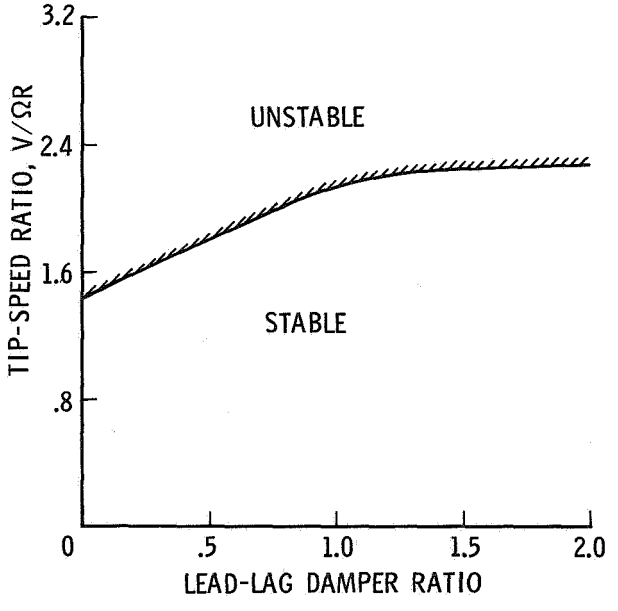

Figure 8.- Effect of lead-lag hinge damping restraint.

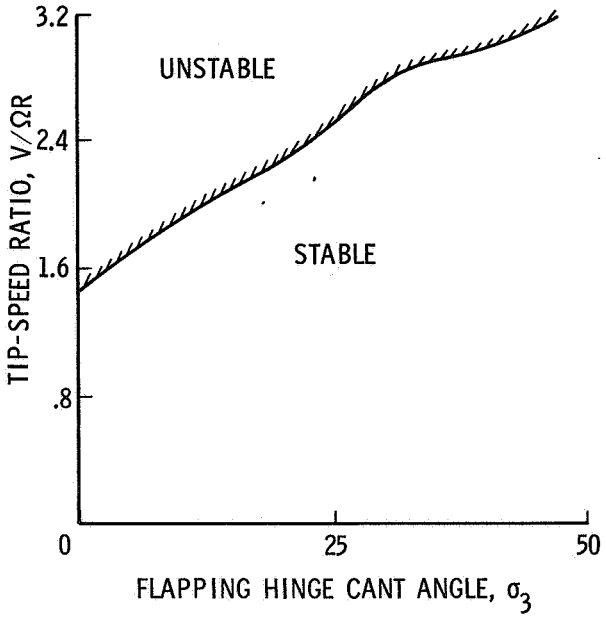

Figure 9.- Effect of flapping hinge cant.

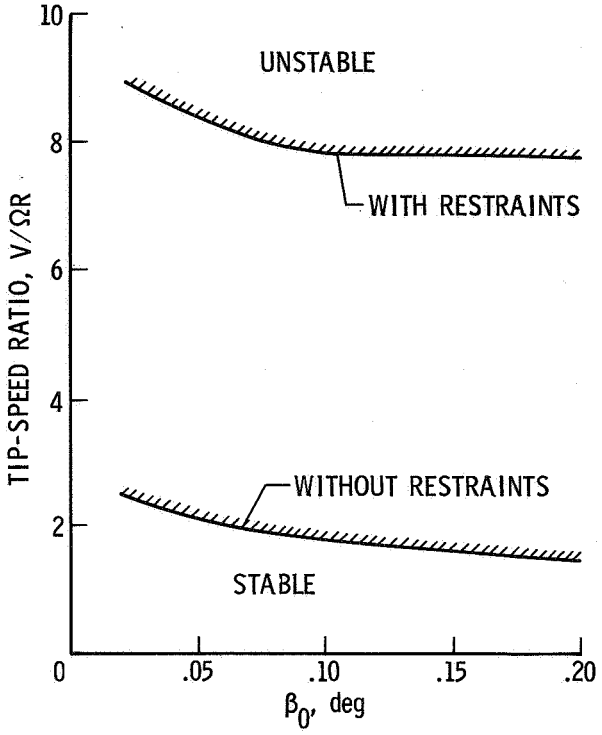

Figure 10.- Effect of combined restraints on blade-motion divergence.

Figure 11.- Flapping-amplitude response to a step input.

NASA-Langley, 1968